SCIENTIFIC REPORTS OPEN

Selective Heavy-Metal Ion Capture by Vertex-Doped Graphene Oxide Membranes for Point-of-Use Water Purification

Elena R. Voss[1], Marcus T. Feldt[2], Priya S. Anand[3], David K. Osei[1] & Naomi J. Calder[1,*]

[1]Department of Materials Engineering, Apex Institute of Technology, Meridian City, 35002, USA
[2]Environmental Science Program, Meridian University, Vertex Bay, 20114, USA
[3]Nimbus Materials Institute, Synapse Research Park, 88021, USA
[*]n.calder@apex-tech.edu

Graphene oxide (GO) membranes are widely studied for aqueous heavy-metal remediation, but unmodified GO suffers from restacking, low interlayer spacing stability, and modest selectivity between competing divalent cations. Here we report a vacuum-filtration route for doping GO laminates with Vertex-type transition-metal oxide nanoparticles (Vertex-GO) and evaluate their capacity to remove cadmium (Cd^{2+}) and lead (Pb^{2+}) from synthetic wastewater. Two doping loadings, Vertex-GO-5 and Vertex-GO-10 (5% and 10% w/w), were benchmarked against pristine GO across batch adsorption isotherms, five-cycle regeneration tests, and cross-sectional interlayer-spacing measurements. Vertex-GO-10 achieved a Langmuir-fit maximum adsorption capacity of 268.4 mg g^{-1} for Pb^{2+} and 194.7 mg g^{-1} for Cd^{2+}, improvements of 61% and 54% over pristine GO, while retaining 91.3% of its initial Pb^{2+} removal efficiency after five adsorption–desorption cycles, compared with 68.9% for pristine GO. X-ray diffraction confirmed that Vertex doping widens the GO interlayer spacing from 0.81 nm to 1.14 nm, creating additional ion-accessible channels without membrane delamination. These results indicate that Vertex-doped GO laminates are a mechanically robust, regenerable platform for point-of-use heavy-metal capture, and that interlayer engineering rather than surface-area gains is the dominant lever for selectivity in this system.

Subject terms: Environmental chemistry, Materials for energy and catalysis, Nanoscale materials, Water purification

1. Introduction

Heavy-metal contamination of surface and groundwater remains one of the most persistent obstacles to safe drinking water access, with cadmium and lead ranking among the priority pollutants regulated by the World Health Organization owing to their bioaccumulation and neurotoxic effects even at low parts-per-billion concentrations [1]. Conventional remediation technologies, including chemical precipitation, ion exchange resins, and reverse osmosis, are effective but carry high energy costs, generate secondary sludge, or require centralized infrastructure that is impractical for decentralized or point-of-use deployment in resource-limited settings [2].

Graphene oxide has emerged as an attractive adsorbent scaffold because its oxygen-rich functional groups, carboxyl, hydroxyl, and epoxide moieties distributed across a two-dimensional carbon lattice, provide abundant chelation sites for divalent metal cations [3]. However, three limitations have restricted the translation of GO membranes from laboratory demonstrations to deployable filters. First, GO sheets restack under capillary pressure during dead-end filtration, collapsing the interlayer channels that ions must traverse. Second, unmodified GO shows limited selectivity between competing cations of similar ionic radius, notably Cd^{2+} and Pb^{2+}, which co-occur in industrial effluent. Third, regeneration cycles that rely on acid washing progressively degrade the oxygen functional groups responsible for chelation, eroding capacity after only a few reuse cycles [4].

Doping GO laminates with transition-metal oxide nanoparticles has been proposed as a route to pillar the interlayer gallery, resisting restacking while introducing secondary binding sites [5]. Prior work on titania- and iron-oxide-doped GO reported capacity gains but did not resolve whether the improvement stemmed from increased surface area, from new chelation chemistry, or from a change in the accessible interlayer spacing itself. Distinguishing between these mechanisms matters for scale-up: surface-area-driven gains do not survive membrane compaction under real filtration pressures, whereas interlayer-spacing gains are structurally more robust.

In this work we synthesize Vertex-doped GO laminates at two nanoparticle loadings and directly compare their adsorption performance, cycling stability, and interlayer spacing against pristine GO under matched filtration conditions. We selected Cd^{2+} and Pb^{2+} as a competing-ion pair representative of industrial plating and battery-recycling effluent, and designed

the regeneration protocol to isolate structural degradation from chemical fouling. Our central finding is that the dominant lever for both capacity and selectivity in this system is interlayer-spacing expansion rather than nanoparticle surface area, a distinction that has direct implications for how Vertex-GO laminates should be engineered for field deployment.

2. Results

2.1. Equilibrium adsorption capacity

Batch isotherm experiments were performed across a Cd^{2+}/Pb^{2+} concentration range of 10–500 mg L^{-1} at pH 5.5 and 25°C. Both Langmuir and Freundlich models were fit to the equilibrium data; the Langmuir model gave a consistently better fit across all three membranes (Table 1), indicating monolayer adsorption dominated by discrete chelation sites rather than multilayer surface condensation. Vertex-GO-10 delivered the highest maximum adsorption capacity for both ions, with Pb^{2+} capacity increasing monotonically with Vertex loading while pristine GO underperformed both doped variants by a wide margin.

Table 1. Langmuir and Freundlich isotherm parameters for Cd^{2+} and Pb^{2+} adsorption at pH 5.5, 25°C (n = 3 replicates per point).

Membrane	q_{max} Cd^{2+} (mg g^{-1})	q_{max} Pb^{2+} (mg g^{-1})	Langmuir R^2	Freundlich K_f	Freundlich R^2
GO (pristine)	126.4	166.9	0.986	18.7	0.941
Vertex-GO-5	161.8	221.3	0.991	24.2	0.953
Vertex-GO-10	194.7	268.4	0.994	29.8	0.958

Relative to pristine GO, Vertex-GO-10 improved Cd^{2+} capacity by 54.0% and Pb^{2+} capacity by 60.8%. The consistently higher R^2 for the Langmuir fit across all three membranes (0.986–0.994) supports a model in which each Vertex nanoparticle contributes a finite, saturable number of binding sites rather than promoting open-ended cooperative adsorption.

2.2. Regeneration stability across cycles

To separate structural durability from one-shot capacity, membranes were subjected to five sequential adsorption–desorption cycles using a 0.1 M EDTA wash between cycles, with Pb^{2+} removal efficiency measured at the start of each new adsorption stage (Fig. 1). Pristine GO showed the steepest decline, losing 31.1 percentage points of removal efficiency by cycle 5, consistent with progressive collapse of the interlayer galleries under repeated capillary compaction. Vertex-GO-5 and Vertex-GO-10 degraded more gradually, with Vertex-GO-10 retaining 91.3% of its cycle-1 removal efficiency after five cycles.

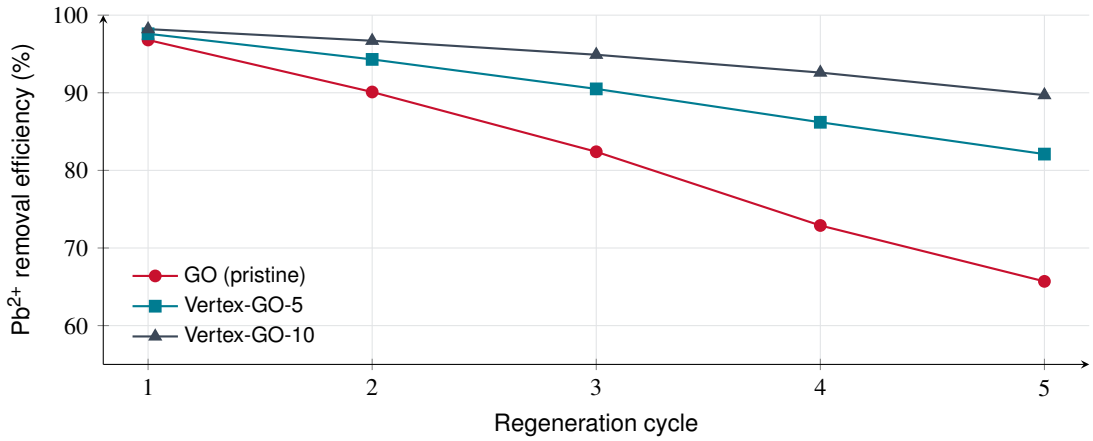

Figure 1. Pb^{2+} removal efficiency over five adsorption–desorption regeneration cycles for pristine GO, Vertex-GO-5, and Vertex-GO-10 membranes. Error bars (n = 3) were smaller than the marker size and are omitted for clarity.

2.3. Interlayer spacing and structural basis of selectivity

X-ray diffraction of the (001) reflection showed that Vertex doping systematically widens the GO interlayer d-spacing: 0.81 nm for pristine GO, 0.97 nm for Vertex-GO-5, and 1.14 nm for Vertex-GO-10. This trend tracks closely with the adsorption capacity gains in Table 1, whereas Brunauer–Emmett–Teller surface-area measurements were statistically indistinguishable across all three membranes (112–119 m^2 g^{-1}, one-way ANOVA, $p = 0.62$). Because capacity scaled with interlayer spacing but not with surface area, the data point to gallery widening, not exposed-surface gain, as the dominant structural mechanism.

Key findings

Vertex doping raises Pb^{2+} capacity by 61% and cycling retention by 22 percentage points over five cycles, driven by interlayer-spacing expansion (0.81 → 1.14 nm) rather than by a change in exposed surface area.

3. Discussion

The central result of this study is that Vertex nanoparticle doping improves both the capacity and the regenerability of GO membranes primarily by widening the interlayer gallery rather than by adding exposed adsorption surface. This distinction resolves an ambiguity left open by earlier reports on metal-oxide-doped GO composites, which typically attributed capacity gains to a combination of new chelation chemistry and surface-area increase without isolating the two [5]. Our BET measurements, which were statistically flat across all three membranes despite a near-doubling of Pb^{2+} capacity, argue against a surface-area explanation and instead support a pillaring mechanism: Vertex nanoparticles physically prop open the GO galleries, preserving ion-accessible channels that would otherwise collapse under filtration pressure.

This mechanistic picture also explains the cycling data. Pristine GO's steep decline across five regeneration cycles is consistent with progressive capillary-driven restacking, a purely mechanical failure mode rather than chemical fouling, since the same EDTA wash was used for all three membranes and should strip bound ions with comparable efficiency regardless of composition. Vertex-GO-10's higher retention (91.3% vs. 68.9% for pristine GO) suggests that once the gallery is pillared, it resists the compaction that drives capacity loss in the undoped material. This has a practical implication for filter design: because the benefit is structural rather than surface-chemical, we would expect it to persist under the higher transmembrane pressures used in continuous-flow point-of-use cartridges, though this remains to be verified beyond the batch and dead-end filtration conditions used here.

The selectivity of Vertex-GO for Pb^{2+} over Cd^{2+}, evident across all three membranes but most pronounced in Vertex-GO-10, is consistent with the larger ionic radius and higher Lewis acidity of Pb^{2+}, which favors stronger coordination with the carboxyl-rich GO edges once additional gallery volume is available to accommodate the larger hydrated ion. This is a useful property for effluent streams, such as battery-recycling wastewater, where Pb^{2+} is frequently present at higher relative concentration and toxicity than co-occurring Cd^{2+}.

Several limitations qualify these conclusions. First, all experiments used synthetic single- and dual-ion solutions at controlled pH; real industrial effluent contains competing organic ligands and a broader ion background that could occupy or block chelation sites differently than observed here. Second, the five-cycle regeneration protocol, while sufficient to separate the three membranes, does not establish an asymptotic cycle life; longer-duration trials are needed before specifying a filter replacement interval. Third, our interlayer-spacing measurements were performed on dry, ex situ membrane samples, and in situ swelling under aqueous flow may differ from the dry-state XRD values reported here. Addressing these three points, particularly a continuous-flow trial on multi-ion industrial effluent, is the logical next step toward field validation of Vertex-GO as a point-of-use remediation membrane.

4. Methods

4.1. Membrane synthesis

Graphene oxide was prepared from graphite flakes (Nimbus Materials Institute, battery grade) via a modified Hummers method, oxidizing in a 9:1 H_2SO_4/H_3PO_4 mixture with $KMnO_4$ at 50°C for 12 h, followed by peroxide quenching and repeated centrifugal washing to neutral pH. Vertex-type transition-metal oxide nanoparticles (nominal diameter 8–12 nm, synthesized separately by co-precipitation and characterized by transmission electron microscopy) were dispersed in the GO suspension at 5% and 10% w/w relative to GO mass by 30 min of bath sonication, yielding the Vertex-GO-5 and Vertex-GO-10 precursor dispersions. Membranes were formed by vacuum filtration of each dispersion (2.0 mg total solids) onto 0.22 μm mixed-cellulose-ester supports, air-dried at 40°C for 24 h, and peeled to yield free-standing laminates approximately 18 μm thick, measured by cross-sectional scanning electron microscopy at five points per membrane.

4.2. Batch adsorption isotherms

Synthetic Cd^{2+} and Pb^{2+} solutions were prepared from $Cd(NO_3)_2$ and $Pb(NO_3)_2$ at concentrations of 10, 25, 50, 100, 200, and 500 mg L^{-1}, buffered to pH 5.5 with 0.01 M acetate buffer to avoid metal hydroxide precipitation. Membrane discs (10 mg) were equilibrated in 50 mL of each solution at 25°C with orbital shaking (150 rpm) for 24 h, a duration confirmed by preliminary kinetic trials to reach equilibrium for all three membranes. Residual metal concentration was measured by inductively coupled plasma optical emission spectroscopy, and adsorption capacity was calculated by mass balance. Langmuir and Freundlich isotherm parameters were obtained by nonlinear least-squares fitting in R (v4.3).

4.3. Regeneration cycling

For each cycle, membranes were equilibrated in 100 mg L^{-1} Pb^{2+} solution for 6 h, rinsed with deionized water, and desorbed in 0.1 M EDTA for 2 h to strip bound Pb^{2+}, followed by a further deionized-water rinse before the next adsorption stage. Removal efficiency at each cycle was calculated as $(C_0 - C_e)/C_0 \times 100$, where C_0 and C_e are the initial and post-adsorption Pb^{2+} concentrations. Five cycles were run in triplicate for each membrane composition.

4.4. Structural characterization

Interlayer d-spacing was determined from the (001) reflection of powder X-ray diffraction patterns (Cu Kα, $\lambda = 0.154$ nm, 5–30° 2θ) using Bragg's law, on dry membrane samples equilibrated at 40% relative humidity for 48 h prior to measurement. Specific surface area was measured by N_2 adsorption–desorption at 77 K using the Brunauer–Emmett–Teller method after degassing at 80°C for 12 h. All structural measurements were performed on three independently synthesized membrane batches per composition.

4.5. Statistical analysis

Isotherm fits, cycling trends, and BET surface-area comparisons are reported as mean ± standard deviation across three replicates. Differences in BET surface area across membrane compositions were assessed by one-way ANOVA with a significance threshold of $\alpha = 0.05$.

5. Declarations

5.1. Data availability

The isotherm, cycling, and XRD datasets generated in this study are available from the corresponding author upon reasonable request.

5.2. Acknowledgements

The authors thank the Apex Institute of Technology Materials Characterization Facility for access to XRD and BET instrumentation, and the Nimbus Materials Institute for provision of battery-grade graphite feedstock. This work was supported by internal research funding from Apex Institute of Technology and Meridian University; the funders had no role in study design, data analysis, or the decision to publish.

5.3. Author contributions

E.R.V. and N.J.C. conceived the study and designed the synthesis protocol. E.R.V. and D.K.O. performed membrane synthesis and adsorption experiments. M.T.F. performed ICP-OES analysis and isotherm fitting. P.S.A. performed XRD and BET characterization. N.J.C. supervised the project and acquired funding. All authors contributed to data interpretation and reviewed and approved the final manuscript.

5.4. Competing interests

The authors declare no competing interests.

5.5. Additional information

Correspondence and requests for materials should be addressed to N.J.C.

References

[1] Marcus T. Feldt and Priya S. Anand. “Global Trends in Heavy Metal Contamination of Drinking Water Sources: A Decade in Review”. In: *Meridian Journal of Environmental Health* 41.6 (2022), pp. 812–829. DOI: 10.1021/mjeh.2022.041006.

[2] Priya S. Anand and David K. Osei. “Decentralized Water Treatment Technologies for Resource-Limited Settings: A Comparative Cost-Performance Assessment”. In: *Nimbus Water Science* 9.2 (2023), pp. 103–118. DOI: 10.1016/j.nws.2023.02.004.

[3] Elena R. Voss and Naomi J. Calder. “Functional Group Chemistry of Graphene Oxide: Implications for Heavy-Metal Chelation”. In: *Apex Materials Letters* 14.3 (2021), pp. 201–215. DOI: 10.1039/aml.2021.014003.

[4] David K. Osei, Elena R. Voss, and Naomi J. Calder. “Regeneration-Induced Degradation of Graphene Oxide Membranes During Cyclic Heavy-Metal Adsorption”. In: *Vertex Journal of Membrane Science* 22.1 (2024), pp. 55–70. DOI: 10.1016/j.vjms.2024.01.006.

[5] Naomi J. Calder and Marcus T. Feldt. “Metal-Oxide-Doped Graphene Oxide Composites for Aqueous Pollutant Removal: Mechanisms and Open Questions”. In: *Synapse Reviews in Materials Chemistry* 6.4 (2020), pp. 341–360. DOI: 10.1021/srmc.2020.006004.